Real-time trajectory generation technique for dynamic soaring UAVs

Naseem Akhtar * **James F Whidborne** * **Alastair K Cooke** *

* *Department of Aerospace Sciences, Cranfield University, Bedfordshire MK45 0AL, UK. email:*n.akhtar@cranfield.ac.uk

Abstract: This paper addresses the problem of generating real time trajectories for dynamic soaring of UAVs (unmanned aerial vehicles). The UAVs soar using the wind shear available over the oceans. The UAVs utilize the energy from low-altitude wind gradients to reduce fuel consumption. For a propeller driven UAV, a performance index is selected to minimize the average power required per cycle of powered dynamic soaring with variable power. The control problem is formulated by considering the UAV equations of motion, operational constraints, initial conditions and terminal conditions that enforce a periodic flight. The differential flatness property of the equations of motion is used to transform the problem to the output space, which permits rapid solution using standard nonlinear programming. The results obtained are compared with those achieved for a collocation technique and a constrained optimization technique.

Keywords: Real time trajectory generation, direct method, dynamic soaring, differential flatness, inverse dynamics.

NOTATION

β	Wind gradient.
K	Induced drag factor.
E_{max}	Aerodynamic efficiency.
C_L	Lift Coefficient.
C_D	Drag Coefficient.
C_{D_0}	Zero lift drag coefficient.
x, y, h	Position relative to Earth axis.
V	Velocity.
m	Mass.
g	Acceleration due to gravity.
γ	Flight path angle.
ϕ	Bank Angle.
ψ	Heading Angle.
$\bar{(\cdot)}$	Normalized states.
t_f	final time.
n	Load factor.
$a_{x_{0\ldots7}}$	Coefficients of the polynomial.
τ	Virtual arc.
λ	Speed factor.
ρ	Air density.
$\bar{\rho}$	Normalized wind conditioning parameter.

1. INTRODUCTION

The extraction of energy from low-level wind gradients is called dynamic soaring [Zhao, 2004b]. The purpose of dynamic soaring is to allow UAVs to increase endurance. In a typical pattern of dynamic soaring a bird would descend with the prevailing wind to gain airspeed. On getting close to the sea surface, it turns into wind and begins to climb. Although the forward advance decreases due to the climb the bird maintains sufficient lift due to increased speed provided by the wind gradient. When the peak wind velocity is reached the bird changes direction to descend and starts the process again. It is possible, if the wind gradient is steep enough, for the bird to extract sufficient energy to maintain flight without flapping [Zhao, 2004b].

Optimal control methods have been used by Zhao [2004b] to minimize either the average power per cycle or the level of constant power required by a propeller driven UAV. The real time determination of the optimal flight patterns would allow the exploitation of dynamic soaring for fuel efficient UAV applications.

Powered UAV dynamic soaring flight through wind gradient can be formulated as a non-linear optimal control problem [Zhao, 2004b,a] has generated solutions for both linear and nonlinear wind gradient profiles. A three-dimensional point mass model is used. In the case of a linear wind profile [Zhao, 2004b], through normalization of the UAV equations of motion, a single parameter has been defined that represents the relative wind effect on the UAV. Performance indices are selected to minimize the average power required per cycle with either variable or constant power. These optimal control problems are converted into parameter optimization with a collocation technique and solved numerically.

Sachs & da Costa [2003] have also studied the problem of energy extraction from wind shear using optimization techniques. Deittert et al. [2006] includes a review of the art of dynamic soaring. The dynamic soaring equations are derived and solved and the results are discussed with respect to generic UAV models.

⋆ This work was supported by BAE Systems and EPSRC.

The optimization approach used in this paper is based on the Direct Method of Taranenko [Yakimenko, 2000]. This method permits the solution of trajectory optimization problems in the output space. Control histories are obtained by dynamic inversion without any requirement to solve the integral equations. It should be noted that the use of a virtual time argument allows the temporal and spacial requirements to be decoupled. As the method is very efficient it is able to find near-optimal trajectories rapidly enough to allow real-time implementation [Yakimenko, 2000] thereby allowing the exploitation of dynamic soaring for fuel efficient UAV operations.

In the next section, the vehicle and wind models are given and in Section 3 the inverse dynamic equations are presented. Section 4 describes the Direct Method and its application to the dynamic soaring problem. In Section 5 the results are presented and compared with those from Zhao [2004b] and some obtained using a simple constrained optimization approach.

2. DYNAMIC SOARING MODEL

In a wind gradient field, the horizontal component increases with altitude and wind gradients occur across various altitude ranges. Typically, reasonably stable conditions exist close to the sea surface with the wind velocity nearly zero at the surface and increasing gradually with altitude. Only the horizontal wind is considered. It is assumed that this component is static being a function of altitude only. The linear wind profile can be described as:

$$W_x(h) = \beta h. \tag{1}$$

The values of β for various wind conditions are defined in Zhao [2004b]. The UAV equations can be represented by a three dimensional point mass model in a stationary flat earth reference system [Zhao, 2004b]. The equations of motion are given by:

$$m\dot{V} = T - D - mg\sin\gamma - m\dot{W}_x\cos\gamma\sin\psi \tag{2}$$

$$mV\cos\gamma\dot{\psi} = L\sin\phi - m\dot{W}_x\cos\psi \tag{3}$$

$$mV\dot{\gamma} = L\cos\phi - mg\cos\gamma + m\dot{W}_x\sin\gamma\sin\psi \tag{4}$$

$$\dot{h} = V\sin\gamma \tag{5}$$

$$\dot{x} = V\cos\gamma\sin\psi + W_x(h) \tag{6}$$

$$\dot{y} = V\cos\gamma\cos\psi \tag{7}$$

It is assumed that the UAV mass is constant. The state variables are $[V, \psi, \gamma, x, y, h]$ and the control variables are $[C_L, \mu, T]$. The lift and drag forces are represented as

$$L = \frac{1}{2}\rho V^2 S C_L \tag{8}$$

$$D = \frac{1}{2}\rho V^2 S C_D \tag{9}$$

and

$$C_D = C_{D_0} + KC_L^2 \tag{10}$$

The induced drag factor can be determined from the aerodynamic efficiency E_{max} and the zero lift drag coefficient C_{D_0} as:

$$K = \frac{1}{4E_{max}^2 C_{D_0}}, \tag{11}$$

where

$$E_{max} = \left(\frac{C_L}{C_D}\right)_{max} = \left(\frac{C_L}{C_{D_0} + KC_L^2}\right)_{max}. \tag{12}$$

The above equations of motion are then normalized as follows:

$$\bar{V} = \frac{\beta}{g}V, \qquad \bar{x}, \bar{y}, \bar{h} = \frac{\beta^2}{g}(x, y, h), \tag{13}$$

$$\bar{T} = \frac{T}{mg}, \qquad \tau = \beta t, \tag{14}$$

and we have

$$(\cdot)' = \frac{d(\cdot)}{d\tau} = \frac{1}{\beta}\frac{d(\cdot)}{dt}. \tag{15}$$

The normalized equations of motion are then obtained as [Zhao, 2004b]

$$\bar{V}' = \bar{T} - \bar{\rho}\bar{V}^2(C_{D_0} + KC_L^2) - \sin\gamma - \bar{V}\sin\gamma\cos\gamma\sin\psi, \tag{16}$$

$$\psi' = \bar{\rho}\bar{V}C_L\cos\mu - \tan\gamma\cos\psi, \tag{17}$$

$$\gamma' = \bar{\rho}\bar{V} - \frac{\cos\gamma}{\bar{V}} + \sin^2\gamma\sin\psi, \tag{18}$$

$$\bar{h}' = \bar{V}\sin\gamma, \tag{19}$$

$$\bar{x}' = \bar{V}\cos\gamma\sin\psi + \bar{h}, \tag{20}$$

$$\bar{y}' = \bar{V}\cos\gamma\cos\psi. \tag{21}$$

Note that for presentation of the simulation results, the normalized equations are multiplied by t_f. The wind parameter is defined as

$$\bar{\rho} = \frac{\rho g^2}{2(mg/S)\beta^2}. \tag{22}$$

3. DIFFERENTIAL FLATNESS

Differential flatness is the property of the system that allows one to describe state and controls in terms of outputs and their derivatives. For a system to be differentially flat and therefore possessing a flat output, it requires a set of variables such that:

(1) Every system variable may be expressed as a function of the output $\mathbf{y}$;
(2) Conversely every component of $\mathbf{y}$ may be expressed as a function of the system variables and of a finite number of time derivatives.

By manipulating the equations of motion, the state and input vector can be expressed as a function of the output vector. The outputs of the system are x, y, and h and the inputs are $\bar{T}$, C_L and μ. This gives the inverse dynamics as

$$V = \sqrt{\dot{x}^2 + (\dot{y} - \beta\dot{h})^2 + \dot{h}^2}, \tag{23}$$

$$\gamma = \arcsin\frac{\dot{h}}{V}, \tag{24}$$

$$\psi = \text{atan2}((\dot{y} - \beta m\dot{h}), \dot{x}), \tag{25}$$

$$\dot{\gamma} = \frac{\ddot{h}}{\sqrt{V - \dot{h}^2}} - \frac{\dot{h}(\dot{x}\ddot{x} + (\dot{y} - \beta\dot{h})(\ddot{y} - \beta\ddot{h})) + \dot{h}\ddot{h}}{V^2\sqrt{V - \dot{h}^2}}, \tag{26}$$

$$\dot{\psi} = \frac{\dot{x}(\ddot{y} - \beta\ddot{h}) - (\dot{y} - \beta\dot{h})\ddot{x}}{\dot{x} + (y - \beta\dot{h})^2}, \tag{27}$$

$$\bar{T} = \bar{V}' + \rho\bar{V}^2(C_{D0} + KC_2^2) + \sin\gamma + \bar{V}\sin\gamma\cos\gamma\sin\psi, \tag{28}$$

$$\mu = \arctan\cos\gamma\frac{\psi' + \tan\gamma\cos\gamma}{\gamma' + (\cos\gamma)/\bar{V} - \sin^2\gamma\sin\psi}, \tag{29}$$

$$C_L = \frac{\bar{V}\gamma' + \cos\gamma - \bar{V}\sin^2\gamma\sin\psi}{\bar{\rho}\bar{V}^2\cos\mu}. \tag{30}$$

4. THE DIRECT METHOD OF TARANENKO

This is a non-linear constrained optimization method where some reference polynomials are determined by the boundary conditions. The speed profile can be separated from trajectory by introduction of a virtual arc instead of time. The inequality constraints are direct functions of the output due to differential flat properties of the system, which helps to speed-up the process for on-board implementation. For further details, see Yakimenko [2000] and Whidborne et al. [2008].

4.1 Parametrization

The trajectories are dependent on the coefficients of the polynomials that define the trajectories. The coefficients are determined analytically from the known boundary conditions, that is the initial & final positions, velocities & accelerations and the free variables which are taken as the initial & final jerks 9derivatives of accelerations) and the final time. The degree of the reference polynomials is given by the number of boundary conditions that have to be met to calculate all the coefficients. The minimum degree of the polynomial must be equal to $n = d_0 + d_f + 1$ with $d_{0,f}$ being the maximum order of the time derivative of the UAV coordinates. If the initial and final acceleration coordinates are preset ($d_0 = d_f = 2$), the reference polynomial will be fifth order. An addition of one fictive boundary condition ($x^2_{o,f}$) gives a more flexible reference trajectory. These fictive boundary values are added as additional optimization variables. They are free to vary to find more near-optimal solutions. In this case $n = 7$ and this gives us a total of 24 coefficients calculated from

$$a_{x0} = x_0 \tag{31}$$

$$a_{x1} = x_0' \tag{32}$$

$$a_{x2} = x_0'' \tag{33}$$

$$a_{x3} = x_0''' \tag{34}$$

$$a_{x4} = -\frac{2x_f''' + 20x_0'''}{\tau_f} + \frac{30x_f'' - 60x_0''}{\tau_{f^2}''} - \frac{180x_f' + 240x_0'}{\tau_{f^3}} + 420\frac{x_f - x_0}{\tau_{f^4}} \tag{35}$$

$$a_{x5} = -\frac{10x_f''' + 20x_0'''}{\tau_{f^2}} + \frac{140x_f'' - 200x_0''}{\tau_{f^3}''} - \frac{780x_f' + 900x_0'}{\tau_{f^4}} + 420\frac{1020x_f + 1080x_0}{\tau_{f^5}}, \tag{36}$$

$$a_{x6} = -\frac{15x_f''' + 20x_0'''}{\tau_{f^3}} + \frac{195x_f'' - 225x_0''}{\tau_{f^4}''} - \frac{1020x_f' + 1080x_0'}{\tau_{f^5}} + 2100\frac{x_f - x_0}{\tau_{f^6}}, \tag{37}$$

$$a_{x7} = -7\frac{x_f''' + x_0'''}{\tau_{f^4}} - 84\frac{x_f'' - x_0''}{\tau_{f^5}''} + 420\frac{x_f' + x_0'}{\tau_{f^5}} + 420\frac{x_f - x_0}{\tau_{f^6}} - 840\frac{x_f - x_0}{\tau_{f^7}}, \tag{38}$$

where τ_f is the final value of the individual arc, and is free parameter of the optimization. The reference function is then

$$x(\tau) = \sum_{k=0}^{7}\frac{a_{xk}\tau^k}{\max(1, k(k-1))}; \tag{39}$$

The process is identical for the two other coordinates, y and h.

4.2 The Virtual Arc

The use of a virtual arc, τ, enables the speed profile to be separated from the trajectory [Etchemendy, 2007] i.e. the velocity can be independently varied from the reference trajectory. Therefore a UAV can follow the same trajectory with different speed histories. If we set $\tau = t$ then the speed is fixed and equal to

$$V = \sqrt{\dot{x}^2 + \dot{y}^2 + \dot{h}^2}. \tag{40}$$

The virtual arc is linked to the time by the variable speed parameter, λ, which allows us to vary speed along the trajectory. The speed is then

$$V = \lambda\sqrt{x'^2 + y'^2 + h'^2}. \tag{41}$$

4.3 The Optimization Problem

The differential flatness properties allow us to set the optimization problem in the output space [Cowling et al., 2007]:

$$\min\left\{\Phi : \mathbf{y}(t) \in \mathbb{R}^3, t \in [0, t_f]\right\}, \tag{42}$$

such that:

$$d(y) \leq 0. \tag{43}$$

where ϕ is the cost function and represents the value to be minimized and $d(y)$ represents the constraints. d is only a function of the output (& its derivatives) and it reduces the computation time. The problem has been programmed in MATLAB by using the parametrization described and the optimization function `fmincon`.

The cost function is defined as:

$$\Phi(C_L, \mu, \bar{T}, \bar{V}_0, \psi_0, \tau_f) = \frac{1}{\tau_f}\int_0^{\tau_f}\bar{T}\bar{V}d\tau \tag{44}$$

4.4 Constraints

Some constraints are specified to avoid singularities in the dynamic inversion equations. Other constraints are imposed to represent constraints on the control power and the stall speed. The possible singularities are:

$$V = 0, \tag{45}$$
$$\cos(\gamma) = 0, \tag{46}$$
$$\cos(\phi) = 0, \tag{47}$$
$$g\cos(\gamma) + V\dot{\gamma} = 0. \tag{48}$$

Thus all the constraints are:

$$V > 0, \tag{49}$$
$$-90^o < \phi, \gamma < 90^o, \tag{50}$$
$$60 \text{ m/s } < V < 123 \text{ m/s }, \tag{51}$$
$$-30^o < \gamma < 30^o, \tag{52}$$
$$\bar{T} > 0, \tag{53}$$
$$\tag{54}$$

4.5 Inverse dynamics

A numerical solution is obtained by dividing the virtual arc $[0,\ \tau_f]$ into N equally placed points [Cowling et al., 2007]. The interval between he two points is defined as:

$$\Delta\tau = \frac{\tau_f}{N-1} \tag{55}$$

With $\tau_0 = 0$ the next value of the virtual arc is computed as:

$$\tau_j = \tau_{j-1} + \Delta\tau \text{ for } j = 1 \dots N \tag{56}$$

The reference polynomials are found as polynomials of τ and these only depend on the boundary conditions.

The initial conditions are converted from time derivatives to virtual arc derivatives using the following relationship:

$$\lambda(\tau) = \frac{d\tau}{dt} \tag{57}$$

This brings us to the obvious relations:

$$\dot{x} = \frac{dx}{d\tau}\frac{d\tau}{dt} = \lambda x', \tag{58}$$
$$\ddot{x} = \frac{d((\lambda x')}{d\tau}\frac{d\tau}{dt} = \lambda^2 x'' + \lambda\lambda' x', \tag{59}$$
$$\dddot{x} = \frac{d(\lambda^2 x'' + \lambda\lambda' x')}{d\tau}\frac{d\tau}{dt} \tag{60}$$
$$= \lambda^3 x''' + 3\lambda^2\lambda' x'' \qquad + x'(\lambda^2\lambda'' + \lambda\lambda'^2). \tag{61}$$

After rearrangement this leads to the expression of the virtual arc's first and second derivatives of the coordinates:

$$x' = \dot{x}\lambda^{-1}, \tag{62}$$
$$x'' = \ddot{x}\lambda^{-2} - \dot{x}\lambda'\lambda^{-1}. \tag{63}$$

For the boundary, the values of

$$\lambda_{0,f} = V_{0,f}, \tag{64}$$
$$\lambda'_{0,f} = \dot{V}_{0,f}V_{0,f}^{-1}, \tag{65}$$

may be chosen but the scaling of λ does not really matter (allowing the virtual speed and the actual speed to be equal at the boundaries just implies that the virtual arc τ_f will be of the order of the path length). The current time is computed as follows:

$$t_j = t_{j-1} + \Delta t_{j-1} \tag{66}$$

where $\Delta t_{j-1} =$

$$2\frac{\sqrt{(x_j - x_{j-1})^2 + (y_j - y_{j-1})^2 + (h_j - h_{j-1})^2}}{V_j - V_{j-1}}. \tag{67}$$

Therefore the current value of the speed factor is:

$$\lambda_j = \frac{\Delta\tau}{\Delta t_{j-1}}. \tag{68}$$

5. RESULTS

Figures 1 to 9 show the optimal UAV state and control variables. Note that all are within constraints. Figure 1 shows a three dimensional view of the minimum variable power dynamic soaring flight trajectory for β =0.02965/sec which corresponds to $\bar{\rho} = 140$, a wind conditioning parameter that describes the strength of the wind and is defined by (22). The zero lift drag coefficient, C_{D_0}, was set to 0.01 and E_{max} =25 [Zhao, 2004b].

The UAV would first climb into the wind with a positive climbing angle to trade kinetic energy for potential energy. It loses speed as shown in Figure 2 while gaining altitude. After reaching the maximum altitude possible within the constraints, it then dives along the wind using a negative flight path angle to trade potential energy for speed. During simulations it is noted that as the wind condition parameter $\bar{\rho}$ increased, the peak altitude decreases.

The airspeed reaches a minimum at the peak altitude and a maximum at the lowest altitude, see Figure 2. The lowest airspeed corresponds to the peak lift coefficient and maximum bank angles (Figures 5 and 9). The peak normalized thrust occurs around the maximum velocity and is much lower or close to zero for the rest of the cycle, see Figure 4.

This problem has been solved previously by the author using a constrained optimization method. In this case, a solution to the optimization problem has been achieved in 28 seconds however using the method described in this paper reduced the solution time to eight seconds. No data has been presented in Zhao [2004b] regarding the time taken to optimize the trajectory. However it has been stated that the method is not applicable to real time trajectory generation applications suggesting that the solution time is significant.

The peak value of normalized thrust obtained in our case is 0.06 as compared to 0.25 for Zhao [2004b]. Note that the average normalized thrust used is 0.0085.

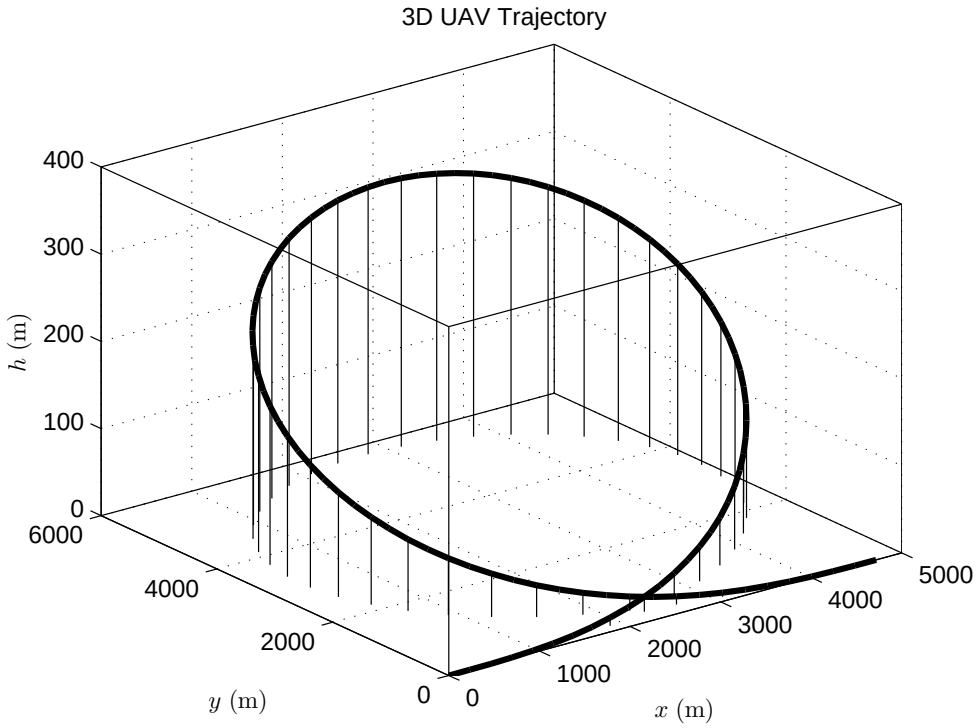

Fig. 1. Optimal trajectory for minimum peak power problem

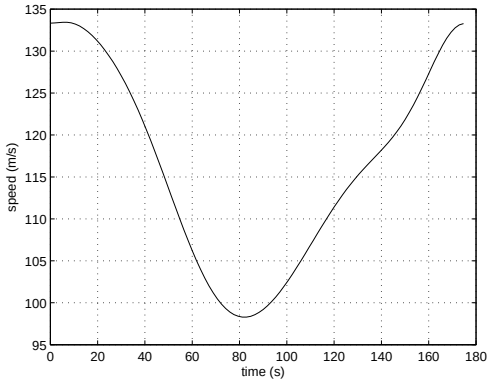

Fig. 2. Speed profile for minimum peak power problem

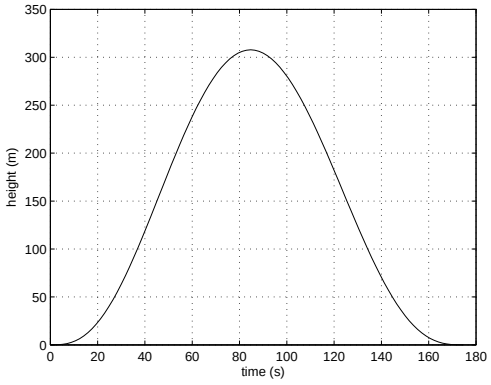

Fig. 3. Height profile for minimum peak power problem

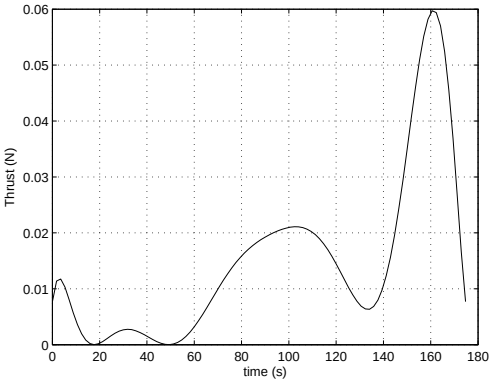

Fig. 4. Thrust profile for minimum peak power problem

6. CONCLUSIONS

The direct method method has a clear advantage over the method of Zhao [2004b] because it could be implemented in real time as the optimization time is just eight seconds compared to a trajectory loop time of 176 seconds. This short time would allow computation of the next loop during the current trajectory loop. Furthermore it predicts a much lower peak thrust requirement suggesting that the UAV will require a smaller sized engine. No direct comparison can be made of average thrust as this information is absent in Zhao [2004b].

Note that results in Zhao [2004b] showed a greater distance in the x direction and also a greater height. The direct method can achieve similar results by increasing the thrust usage.

Results have been obtained for various other values of the wind condition parameter, $\bar{\rho}$, for both the minimum variable power and minimum constant power cost functions. Other cost functions that have been considered are maximum height and minimum time, but the results are not presented here.

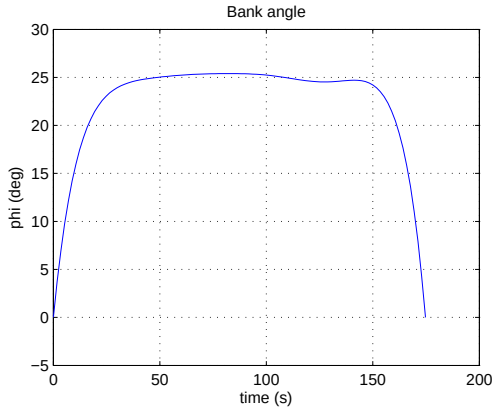

Fig. 5. Bank angle profile for minimum peak power problem

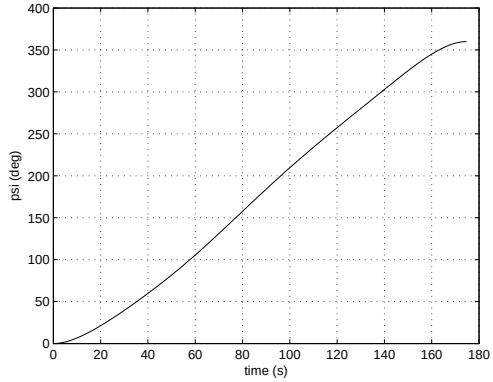

Fig. 6. Heading angle profile for minimum peak power problem

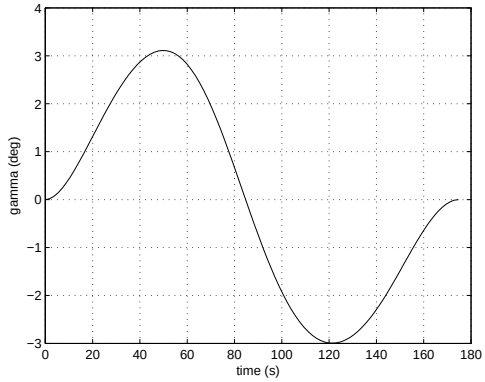

Fig. 7. Climbing angle profile for minimum peak power problem

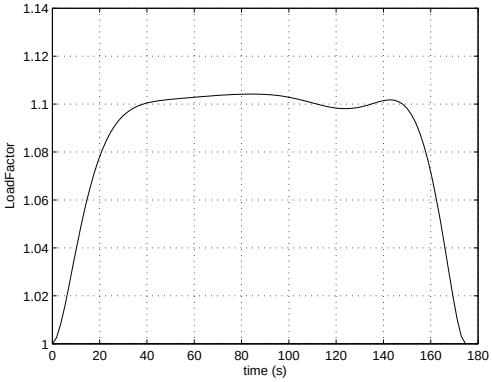

Fig. 8. Load factor profile for minimum peak power problem

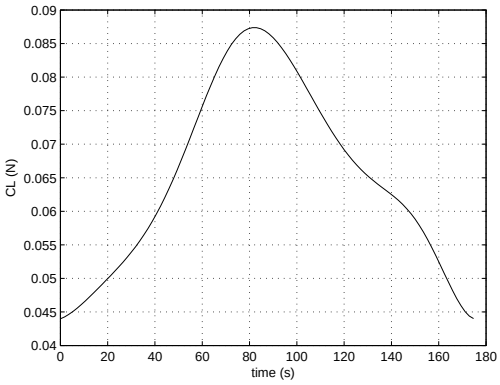

Fig. 9. Lift coefficient profile for minimum peak power problem

REFERENCES

I.D. Cowling, O.A. Yakimenko, J.F. Whidborne, and A.K. Cooke. A prototype of an autonomous controller for a quadrotor UAV. *Proc. European Contr. Conf. 2007*, Kos, Greece, July 2007.

M. Deittert, C. Toomer, A.G. Pipe. Biologically inspired UAV propulsion. *21st Bristol Conference on UAVS*, April 2006

M. Etchemendy, *Flight Control and Optimal Path Planning for UAVs*, MSc Thesis, Cranfield University, 2007

G. Sachs and O. da Costa. Optimization of Dynamic Soaring at Ridges, *AIAA Atmospheric Flight Mechanics Conference and Exhbit*, Austin, Texas, August 2003.

J.F. Whidborne, I.D. Cowling, O.A. Yakimenko. A Direct Method for UAV Guidance and Control. *23rd Bristol Conference on UAVS*, April 2008

O.A. Yakimenko. Direct method for rapid prototyping of near-optimal aircraft trajectories. *J. Guid. Control Dynam.*, 23(5):865–875, 2000.

Y.J. Zhao. Optimal Dynamic Soaring. Optimal Control Applications and Methods. *Optimal Control Applications and Methods*, 25:67-89, 2004

Y.J. Zhao. Minimum fuel powered dynamic soaring of unmanned aerial vehicles utilizing wind gradients. *Optimal Control Applications and Methods*, 25:211-233, 2004